Neurobiology of Stress 13 (2020) 100238

Contents lists available at ScienceDirect

Neurobiology of Stress

journal homepage: www.elsevier.com/locate/ynstr

Disinhibition of somatostatin interneurons confers resilience to stress in male but not female mice

Sarah J. Jefferson [a,c,1], Mengyang Feng [a,c,1], URee Chon [d], Yao Guo [a,c], Yongsoo Kim [d], Bernhard Luscher [a,b,c,*]

[a] Department of Biology, Pennsylvania State University, University Park, PA, 16802, USA
[b] Department of Biochemistry & Molecular Biology, Pennsylvania State University, University Park, PA, 16802, USA
[c] Center for Molecular Investigation of Neurological Disorders (CMIND), The Huck Institutes of the Life Sciences, Pennsylvania State University, University Park, PA, 16802, USA
[d] Department of Neural and Behavioral Sciences, College of Medicine, Pennsylvania State University, Hershey, PA, 17033, USA

ARTICLE INFO

Keywords:
Antidepressant
eEF2
Somatostatin
Neural inhibition
Excitation-inhibition balance

ABSTRACT

Chronic stress represents a vulnerability factor for anxiety and depressive disorders and has been widely used to model aspects of these disorders in rodents. Disinhibition of somatostatin (SST)-positive GABAergic interneurons in mice by deletion of γ2 $GABA_A$ receptors selectively from these cells (SSTCre:$\gamma2^{f/f}$ mice) has been shown to result in behavioral and biochemical changes that mimic the responses to antidepressant doses of ketamine. Here we explored the extent to which SSTCre:$\gamma2^{f/f}$ mice exhibit resilience to unpredictable chronic mild stress (UCMS). We found that male SSTCre:$\gamma2^{f/f}$ mice are resilient to UCMS-induced (i) reductions in weight gain, (ii) reductions in SST-immuno-positive cells in medial prefrontal cortex (mPFC), (iii) increases in phosphorylation of eukaryotic elongation factor 2 (eEF2) in mPFC, and (iv) increased anxiety in a novelty suppressed feeding test. Female SSTCre:$\gamma2^{f/f}$ mice were resilient to UCMS-induced reductions in SST-immuno-positive cells indistinguishably from males. However, in contrast to males, they showed no UCMS effects on weight gain independent of genotype. Moreover, in mPFC of female $\gamma2^{f/f}$ control mice, UCMS resulted in paradoxically reduced p-EF2 levels without stress effects in the SSTCre:$\gamma2^{f/f}$ mutants. Lastly, female SSTCre:$\gamma2^{f/f}$ mice showed increased rather than reduced UCMS induced anxiety compared to $\gamma2^{f/f}$ controls. Thus, disinhibition of SST interneurons results in behavioral resilience to UCMS selectively in male mice, along with cellular resilience of SST neurons to UCMS independent of sex. Thus, mechanisms underlying vulnerability and resilience to stress are sex specific and map to mPFC rather than hippocampus but appear unrelated to changes in expression of SST as a marker of corresponding interneurons.

1. Introduction

Chronic stress is a known risk factor for diverse psychiatric disorders, particularly major depressive disorder (MDD) (Stroud et al., 2011; Treadway et al., 2015). Stress-induced elevations of extracellular glutamate are widely recognized as mediators of the detrimental cellular and behavioral effects of chronic stress and also implicated in the etiology of major depressive disorder (MDD) (Moghaddam and Jackson, 2004; McEwen et al., 2016). Preclinical and clinical evidence points to defects in GABAergic inhibition as mediators of stress vulnerability and causal factors for MDD (Luscher and Fuchs, 2015; Ghosal et al., 2017; Newton et al., 2019). In particular, MDD is associated with reduced expression of somatostatin (SST), a marker representative of about 30% of cortical GABAergic interneurons (Fee et al., 2017). In support of a causative role of SST neuron dysfunction in stress-related neuropsychiatric disorders, rodent models subjected to chronic stress exhibit disproportionate gene expression changes in SST neurons (Lin and Sibille, 2015; Girgenti et al., 2019), while micro-infusion of SST into the brain (Engin et al., 2008), knock out of the SST gene (Lin and Sibille, 2015) and chemogenetic silencing of SST neurons (Soumier and Sibille, 2014) result in altered emotional behavior of mice.

GABAergic interneurons are the principal neurons mediating neural inhibition in the brain. In addition to SST neurons, they include

* Corresponding author. Department of Biology, Penn State University, 301 Life Sciences Building, University Park, PA, 16802, USA.
E-mail address: BXL25@psu.edu (B. Luscher).
[1] Joint first authors.

https://doi.org/10.1016/j.ynstr.2020.100238
Received 27 March 2020; Received in revised form 22 May 2020; Accepted 1 July 2020
Available online 10 July 2020

Abbreviations

129	129X1/SvJ
BL/6J	C57BL/6J
eEF2	eukaryotic elongation factor 2
eEF2K	eukaryotic elongation factor 2 kinase
EPM	elevated plus maze
GABA	γ-aminobutyric acid
$GABA_A$ receptor	Ionotropic GABA receptor
ILC	infralimbic cortex
IP	immuno-positive
MDD	major depressive disorder
mPFC	medial prefrontal cortex
mTOR	mammalian target of rapamycin
NMDA	N-methyl-D-aspartate
NS	no stress
NSFT	novelty suppressed feeding test
OFT	open field test
OLM	oriens lacunosum molecular
PLC	prelimbic cortex
PV	parvalbumin
SPT	sucrose preference test
SSPT	sucrose splash test
SST	somatostatin
STPT	serial two-photon tomography
UCMS	unpredictable chronic mild stress
VIP	vasoactive intestinal peptide
WT	wildtype

interneurons that express the Ca^{2+} binding protein parvalbumin (PV, approximately 40%), or the 5-HT3a receptor (30%) as identifying marker proteins (Rudy et al., 2011). SST neurons are structurally and functionally heterogeneous but they include Martinotti cells in the neocortex and Oriens Lacunosum Moleculare (OLM) and bistratified cells in the hippocampus as major subtypes that specifically target the distal apical dendrites of pyramidal cells (Muller and Remy, 2014; Yavorska and Wehr, 2016). Functionally, these cells provide network activity-dependent supra-linear feedforward inhibition to pyramidal cells (Kapfer et al., 2007; Tan et al., 2008). Their activity scales with network activity in the theta frequency, a property that is also regulated by anxiolytic and antidepressant drugs (McNaughton et al., 2007).

Anxiety and depressive disorders are increasingly recognized to involve chronic imbalances of neural excitation and inhibition due to defects in GABAergic inhibition and excesses in glutamatergic excitation (Luscher and Fuchs, 2015). Reduced GABA levels found in MDD patients are restored by antidepressant drug treatment (Sanacora et al., 2002; Bhagwagar et al., 2004; Kucukibrahimoglu et al., 2009). Studies in rodents indicate that relatively modest, genetically-induced defects in GABAergic inhibition can cause anxiety- and depression-related behavioral changes (Crestani et al., 1999; Earnheart et al., 2007; Vollenweider et al., 2011; Kolata et al., 2018) that are reversible by chronic treatment with the tricyclic antidepressant desipramine (Shen et al., 2010) or with the rapid antidepressant ketamine (Ren et al., 2016). The antidepressant behavioral effects of ketamine in $GABA_A$ receptor ($GABA_AR$)-mutant mice are associated with restoration and potentiation of GABAergic synaptic inhibition of pyramidal cells (Ren et al., 2016). Similarly, chronic stress-induced downregulation of GABAergic synapses can be reversed by ketamine (Ghosal et al., 2020). Collectively, these data suggest that GABA itself may have antidepressant properties.

To test by genetic means whether GABA has antidepressant properties, we recently examined mice with disinhibited SST neurons, using deletion of γ2 $GABA_ARs$ selectively from these neurons (SSTCre:$\gamma2^{f/f}$ mice) (Fuchs et al., 2017). As predicted, SST cells of SSTCre:$\gamma2^{f/f}$ mice were hyperexcitable, resulting in increased GABAergic inhibition of hippocampal and cortical pyramidal cell targets. Consistent with a shift in synaptic excitation:inhibition balance towards greater inhibition (Heise et al., 2016), the circuit changes of SSTCre:$\gamma2^{f/f}$ mice were accompanied by reduced activity of the Ca^{2+} dependent enzyme eukaryotic elongation factor 2 kinase (eEF2K) and reduced phosphorylation of its target, eEF2. Behaviorally, SSTCre:$\gamma2^{f/f}$ mice reproduced the anxiolytic- and antidepressant-like behavior of mice that have been treated with ketamine. Lastly, SST mRNA and protein levels in SSTCre:$\gamma2^{f/f}$ mice remained unaffected, suggesting that the behavioral changes of SSTCre:$\gamma2^{f/f}$ mice can be attributed to increased GABAergic inhibition of pyramidal cells. Collectively, these data indicated that enhancing GABAergic synaptic inhibition of pyramidal cell dendrites through disinhibition of SST neurons reproduces the prolonged synaptic, biochemical and behavioral consequences of ketamine treatment (Fuchs et al., 2017) (reviewed in Luscher et al., 2020). Consistent with a putative neuroprotective mechanism, SST cells have been shown to delimit NMDA receptor mediated Ca^{2+} entry into dendritic spines of pyramidal cells (Chiu et al., 2013), which may attenuate the detrimental effects of excessive or untimely glutamatergic input to these cells (Lau and Tymianski, 2010). However, whether SSTCre:$\gamma2^{f/f}$ mice are further protected from the negative consequences of chronic stress has not yet been explored. Here we have extended our studies to test whether SSTCre:$\gamma2^{f/f}$ male and female mice exhibit resilience to chronic stress, using exposure to unpredictable chronic mild stress (UCMS) as a model.

2. Materials and methods

2.1. Animals

All animal experiments were approved by the Institutional Animal Care and Use Committees (IACUC) of the Pennsylvania State University and conducted in accordance with guidelines of the National Institutes of Health (NIH). SSTCre mice (also known as *Sst$^{tm2.1(cre)Zjh}$*/J, Stock #013044), Ai9 mice (B6.Cg-*Gt(ROSA)26Sor tm9(CAGtdTomato)Hze*/J, Stock No 007909) and C57BL/6J mice (BL/6J, Stock No. 000664) were all obtained from Jackson Laboratory (Bar Harbor, ME, USA). The $\gamma2^{f/f}$ mouse line (*Gabrg2^{tm2Lusc}*/J, Stock No: 016830, Jackson Laboratory) containing *Gabrg2* alleles flanked by lox P sites was generated in house (Schweizer et al., 2003). All mice were backcrossed to the BL/6J strain for five or more generations. To limit interference of the SSTCre allele with emotional behavior, the SSTCre locus was strictly maintained in the heterozygous state (Lin and Sibille, 2015). The mice compared in experiments were produced as littermates, with the SSTCre allele present as a single copy (hemizygous) in male breeders to prevent germ line recombination. Breeding pairs and non-stressed control mice were maintained on a 12:12 h reverse light–dark cycle (lights off at 8AM) with food and water available ad libitum. The mice were genotyped at the time of weaning using PCR of tail DNA and an AccuStart II PCR Genotyping Kit (Quantabio, Beverly, MA, USA) and primers described on the JAX web site or in Schweizer et al. (2003). Biochemical and behavioral analyses of animals were all done with the experimenter blinded to genotype and treatment.

2.2. UCMS protocol

SSTCre:$\gamma2^{f/f}$ and $\gamma2^{f/f}$ littermate mice were separated by genotype and sex at the time of weaning. At 8–10 week of age, they were further divided into no stress (NS) and UCMS groups with balancing for sucrose preference and body weight. UCMS mice were singly housed and subjected to six weeks of UCMS consisting of 1–3 mild stressors/day for varied durations on a random schedule as described (Elizalde et al.,

2008). Stressors included removal of bedding (4–24 h), wet cage floor (30 min), rotating mice among cages, cage tilted at a 45° angle (12–18 h), food or water deprivation (12–18 h), change in light-dark cycle, transfer to 4 °C chilled cage, and shaking home cage on a rotating platform (60 RPM, radius: 0.78 cm, 1 min). All stressors were applied during both light and dark phases. NS mice were housed in groups of 2–4 in a separate room. UCMS was continued throughout behavioral analyses with single housing as the only stressor for the 12 h preceding testing.

2.3. Immunohistochemistry and serial two-photon tomography

Mice were anesthetized with Avertin or isoflurane inhalation and perfused with ice-cold phosphate buffered saline (PBS) followed by 4% paraformaldehyde (PFA) in PBS (pH = 7.4). Brains were postfixed for 6 h or overnight in the same solution at 4 °C. For immunohistochemistry, floating sections (50 μm) were immunostained using rat anti-somatostatin (1:250, MAB354, Millipore, Burlington, MA, USA), rabbit anti-parvalbumin (PV, 1:500, ab11427, Abcam, Cambridge, MA, USA), and guinea pig anti-NeuN (1:1000, ABN90, Millipore) and developed using secondary goat antibodies conjugated to Alexa 647 or 488 (Jackson Immuno Research, West Grove, PA, USA) or Cy3 (Molecular Probes, Eugene, OR, USA). All samples from a given sex were processed in parallel. Single optical sections were imaged using a Zeiss LSM Pascal confocal microscope with a 20x objective with at least 3 images quantified per area of interest and brain using Image J (https://imagej.nih.gov/ij/). The densities of SST- and PV-IP cells were normalized to the density of NeuN-IP cells. For serial two-photon tomography (STPT), the mice were perfused as above and the brains postfixed over-night and then embedded in oxidized agarose and cross-linked in sodium borohydrate buffer solution overnight at 4 °C. Using a TissueCyte 1000, imaging system (Tissuevision), series of images of tdTomato-(tdT)-fluorescent cells were acquired in 12 × 16 XY tiles (X and Y resolution = 1 μm) across 280 serial 50 μm z-sections of each mouse. A custom built algorithm was used to perform stitching, signal detection, image registration, and automatic cell counting in defined anatomical regions throughout the brain as described (Kim et al., 2015, 2017).

2.4. Western blotting

Tissue extracts in 50 mM Tris-HCl (pH 8.0), 150 mM NaCl, 2 mM EDTA, 0.1% sodium dodecyl sulfate, 1% Triton X-100, 1 mM $NaVO_3$, 5 mM NaF and 1X protease inhibitor cocktail (Roche, Basel, Switzerland) were analyzed on 4–12% sodium dodecyl sulfate-polyacrylamide gels, transferred to polyvinylidene difluoride membranes and probed with mouse anti β-tubulin (1:10 000, no. T8328, Sigma-Aldrich, St Louis, MO, USA), rabbit anti-phospho-eEF2 (Thr56) (1:500, no. 2331), and rabbit anti-eEF2 (1:500, no. 2332, Cell Signaling Technology, Danvers, MA, USA). Immunoblots were developed using IRDye secondary antibodies and the protein bands imaged and quantitated using an Odyssey CLx infrared imager (LI-COR, Lincoln, NE, USA).

2.5. Behavioral analyses

NS mice were group housed and subjected to only the minimal handling necessary and subjected to behavioral testing along with UCMS exposed mice. Behavioral tests were conducted by an experimenter blind to genotype, during the first 5 h of the dark phase using two tests per week. All behavioral experiments were performed under red light (except for the Open Field Test (OFT)). The animals were tested two at a time with the sequence and pairing of animals changed randomly between tests. Testing was initiated with an Open Field Test (OFT), followed by NSFT, home cage feeding, Sucrose Preference test (SPT), Elevated Plus maze (EPM), and sucrose splash test (SSPT). For the OFT (Shen et al., 2012; Fuchs et al., 2017), the mice were transferred from the holding room (dark phase) and immediately exposed to an odor-saturated 50 × 50 × 20 cm opaque Plexiglass arena and standard room illumination (75 lx) for 10 min. The total distance traveled over 10 min and the % time spent in the 30 × 30 cm center square during the first 5 min were quantitated using an EthoVision XT video tracking system (Noldus Information Technologies, Leesburg, VA, USA). All other tests were conducted under red light. For the NSFT (Shen et al., 2010; Fuchs et al., 2017), the mice were singly housed for 24 h and food deprived for 18 h before testing. They were transferred to the corner of a Plexiglass arena (50 × 50 × 20 cm) containing three cm of saw dust bedding, with a pellet of rodent chow placed on a white cotton nesting square (6 × 6 × .5 cm) in the center of the arena. The latency to feed was hand-scored with feeding defined as the mouse biting into the chow while resting on its hind paws. Trials were stopped after 10 min, even if no feeding occurred. To assess appetite, three days following the NSFT the mice were singly housed with saw dust bedding and food deprived for 18 h as above and then were given a pre-weighed rodent chow pellet in their home cage during the first 4 h of the dark phase. The chow was weighed again 10 min later and the amount consumed was calculated. For the SPT, the mice were housed in standard open lid cages and trained to drink from 25 mL plastic pipettes (with sealed tops) for 12 h with a choice of water and 0.5% sucrose. The pipette positions were switched at the start and 12 h time point of the total 24 h measuring period. For any given training or testing session, half of the mice had the sucrose pipettes positioned to the left of the water-containing pipettes and for the other half the positions were inverted. For the EPM (Lister, 1987), the mice were placed into the center square of an elevated (40 cm) crossbar with two open and two closed arms (30 × 5 cm), facing a closed arm. The closed arms were surrounded by 20 cm walls of clear Plexiglas. The edges of open arms were raised by 2 mm to minimize accidental falling. The behavior was video recorded for 5 min using an EthoVision XT video tracking system. Mice that fell off the EPM were excluded from analysis. For the SSPT (Isingrini et al., 2010), the mice were singly housed for 24 h, transferred to an empty cage and sprayed on their backs twice with a fixed volume (0.7 mL) of 10% sucrose solution using a 250 mL spray bottle, to stimulate grooming behavior. The mice were immediately returned to their home cage and the grooming frequency and duration recorded manually over 5 min.

2.6. Statistics

Statistical testing was performed using Prism 7 software (Graphpad, La Jolla, CA) or, for 3-way repeated measure ANOVAs, SAS (SAS Institute, Cary, NC 27513). For all data sets, outliers identified using the ROUT method (Prism 7) were discarded. Normal distribution of data was verified using the D'Agostino-Pearson omnibus normality test and group means were compared by 2-way or 3-way ANOVA followed by post hoc Fisher's LSD or Tukey test as indicated in Figure legends.

3. Results

3.1. SST immuno-positive neurons in the mPFC of SSTCre:$\gamma 2^{f/f}$ male and female mice are resilient to the detrimental effects of chronic mild stress

UCMS exposure of mice results in marked neocortical reductions of SST mRNA and protein expression (Lin and Sibille, 2015; Banasr et al., 2017) and corresponding reductions in the density of SST immuno-positive (IP) neurons in hippocampus of UCMS exposed rats (Czeh et al., 2015). To begin to assess whether the anxiolytic- and antidepressant-like phenotype of SSTCre:$\gamma 2^{f/f}$ mice includes resilience to stress-induced loss of SST-IP neurons, we subjected eight to ten week old SSTCre:$\gamma 2^{f/f}$ mice and $\gamma 2^{f/f}$ littermate controls to six weeks of UCMS, followed by quantitation of the density of SST-IP interneurons. NS control mice of both genotypes were analyzed in parallel. Notably and in contrast to previous experiments done with mice on the 129 genetic background (Fuchs et al., 2017), all experiments in the current study were performed with mice backcrossed to the BL/6J strain, which is

more widely used for chronic stress studies of mice. We focused on the mPFC because markers of GABAergic inhibition in this brain area are prominently affected by UCMS (Veeraiah et al., 2014; Czeh et al., 2015; Lin and Sibille, 2015; Ma et al., 2016; Banasr et al., 2017) and strongly implicated in stress-associated affective disorders (Treadway et al., 2015). We performed separate quantitation of cell densities in the prelimbic (PLC) and infralimbic cortex (ILC) to account for differences in SST cell densities (Kim et al., 2017) and neural connectivity (He et al., 2016; Liu and Carter, 2018) of these brain regions. Parvalbumin immuno-positive (PV-IP) interneurons were analyzed in the same sections as an additional reference, and we controlled for variations in total neuron density by normalizing the interneuron density to the density of cells expressing the pan-neuronal marker NeuN. Interestingly, exposure of $\gamma2^{f/f}$ mice (both sexes combined) to UCMS resulted in the predicted reduction in the density of SST-immuno-positive (IP) in both PLC and ILC and neither of these effects were observed in SSTCre:$\gamma2^{f/f}$ littermates (Fig. 1A–C). We observed no effects of UCMS on the density of PV-IP neurons, regardless of genotype (Fig. 1D, E). We observed similar effects when we segregated the data by sex. In males, UCMS resulted in significant downregulation of SST^+ cells in PLC and ILC of $\gamma2^{f/f}$ mice but not SSTCre:$\gamma2^{f/f}$ littermates (Fig. 1F,G). Female mice showed an overall pattern similar to males. That is, UCMS-exposed vs. NS $\gamma2^{f/f}$ female mice showed a reduced density of SST-IP neurons in mPFC (PLC + ILC combined, genotype effect: $F_{1,14} = 35.96$, $p < 0.001$, stress effect: $F_{1,14} = 5.59$, $p = 0.03$, ANOVA; $p = 0.03$, $n = 4$, Fisher's LSD), and no such effect was evident in SSTCre:$\gamma2^{ff/}$mice ($p = 0.41$, $n = 4–6$, Fisher's LSD, data not shown). When the PLC and ILC were analyzed separately, the UCMS effects on SST^+ cell density in $\gamma2^{f/f}$ mice were significant in the ILC (Fig. 1K) while in the PLC the stress effect did not reach significance due to low sample numbers (Fig. 1L). As in males, UCMS exposure had no effects on SST^+ cell densities in SSTCre:$\gamma2^{f/f}$ littermates (Fig. 1J,K) nor on the density of PV^+ neurons, independent of genotype (Fig. 1L,M).

3.2. UCMS-induced reductions in SST-IP cells represent loss of SST expression rather than loss of cells

We next asked whether UCMS-induced reductions in the density of SST-IP cells indicates loss of these cells or merely reduced expression of SST. We genetically labeled SST neurons by crossing SSTCre mice with the Cre reporter Ai9, which enables quantitation of these cells independent of altered SST protein expression in adulthood. We previously showed that deletion of one γ2 allele in SSTCre:$\gamma2^{f/+}$:Ai9 mice does not measurably affect the function of SST neurons, nor does it affect anxiety- and depression-related behavior (Fuchs et al., 2017). Thus, for practical reasons we used SSTCre:$\gamma2^{f/+}$:Ai9 mice for this experiment. Comparison of UCMS exposed and NS SSTCre:$\gamma2^{f/+}$:Ai9 mice by STPT using tdT fluorescence as a marker for SST cells revealed unaltered densities of cells in PLC, ILC as well as ventral hippocampus (Fig. 1N,O). We also found no differences in the density of these cells between UCMS exposed SSTCre:$\gamma2^{f/+}$:Ai9 and UCMS SSTCre:$\gamma2^{f/f}$:Ai9 mice (not shown). Therefore, UCMS-induced reductions in SST-IP cells reflect reduced expression of SST rather than loss of SST^+ neurons.

3.3. UCMS-exposed SSTCre:$\gamma2^{f/f}$ male but not female mice show reduced eEF2 phosphorylation in mPFC

Phosphorylation of $eEF2^{T56}$ by eEF2 kinase has been shown to be increased by chronic mild stress selectively in the PFC but not hippocampus of male rats (Gronli et al., 2012). Conversely, p-eEF2 is reduced (indicative of increased eEF2 activity) by both conventional and rapid-acting antidepressants (Autry et al., 2011; Opal et al., 2014; Zanos et al., 2016) and required for antidepressant behavioral effects of ketamine (Nosyreva et al., 2013). Together these data suggest that p-$eEF2^{T56}$ serves as a biochemical marker of chronic stress sensitivity and antidepressant drug action. We previously showed that basal p-eEF2 levels were reduced in stress-naïve SSTCre:$\gamma2^{f/f}$ mice (129 strain) in both mPFC and hippocampus (Fuchs et al., 2017), which is consistent with the antidepressant-like behavioral phenotype of these mice. Here, we compared the p-$eEF2^{T56}$ levels of NS and UCMS-exposed SSTCre:$\gamma2^{f/f}$ mice and $\gamma2^{f/f}$ controls (BL/6J strain) (Fig. 2). In the hippocampus (pooled sexes), p-eEF2 levels were increased by stress independent of genotype (Fig. 2A). However, no such overall effect was evident in the mPFC (Fig. 2B). The reduced p-eEF2 levels of SSTCre:$\gamma2^{f/f}$ mice previously reported for the 129 strain were replicated here for the BL/6J strain but only in hippocampus of males and mPFC of females (Fig. 2B,F) and not in mPFC of males nor hippocampus of females (Fig. 2D,E). A likely explanation for this is provided in the Discussion.

To test for possible sexually dimorphic effects of stress, we further analyzed the data segregated by sex (Fig. 2C–F). In hippocampus of males, p-eEF2 levels showed a significant stress effect independent of genotype and without stress × genotype interaction (Fig. 2C) indicating lack of resilience to stress in the hippocampus of male SSTCre:$\gamma2^{f/f}$ mice. By contrast, in the mPFC of males p-eEF2 levels showed a significant interaction of stress and genotype. UCMS tended to increase the p-eEF2 level selectively in $\gamma2^{f/f}$ mice, while lowering this parameter in SSTCre:$\gamma2^{f/f}$ littermates. Moreover, p-eEF2 levels were reduced in UCMS SSTCre:$y2^{f/f}$ vs. UCMS $y2^{f/f}$ males. Thus, male SSTCre:$\gamma2^{f/f}$ mice are resilient to chronic stress-induced increases in p-eEF2 in mPFC but not hippocampus.

As in males, the hippocampus of female $\gamma2^{f/f}$ and SSTCre:$\gamma2^{f/f}$ mice showed an overall stress effect independent of genotype and no genotype X stress interaction, indicating lack of resilience to stress in the hippocampus of SSTCre:$\gamma2^{f/f}$ mice (Fig. 2E). Curiously, the mPFC of female mice showed the expected genotype effect combined with a paradoxical stress effect and a stress × genotype interaction (Fig. 2F). More explicitly, UCMS resulted in a paradoxical reduction of p-eEF2 levels in female $\gamma2^{f/f}$ mice that is opposite to stress effects reported in the literature for males (Gronli et al., 2012). However, the reduced p-eEF2 levels in stress-naïve SSTCre:$\gamma2^{f/f}$ vs $\gamma2^{f/f}$ mice (Fig. 2F) confirms the genotype effect previously reported for the 129 strain of these mice albeit only in females and not in males or when the sexes were combined (Fig. 2B,D). A possible explanation for incomplete replication of data across strain backgrounds is provided in the Discussion.

3.4. SSTCre:$\gamma2^{f/f}$ male mice exhibit resilience to UCMS-induced increases in anxiety

Next, we examined whether apparent stress resilience of male SSTCre:$\gamma2^{f/f}$ mice was also evident at the level of age related body weight gain and behavior. Weekly body weights of the mice during UCMS exposure (starting at 8–10 weeks of age) revealed a stress × genotype interaction of weight gain, with UCMS exposed $\gamma2^{f/f}$ mice showing reduced weight gain compared to NS $\gamma2^{f/f}$ controls. By contrast, the weight gain of SSTCre:$\gamma2^{f/f}$ mice remained unaffected by UCMS (Fig. 3B), suggesting that these mice are resilient to the chronic stress effects on weight gain. Importantly, a separate cohort of UCMS and NS WT and SSTCre control mice that was tested analogously revealed reduced weight gains of both UCMS SSTCre and UCMS WT mice compared to their respective NS control groups (Fig. S1A). Thus, unspecific Cre-recombination did not contribute to resilience of SSTCre:$\gamma2^{f/f}$ mice with respect to UCMS-induced reductions in weight gain.

When we analyzed $\gamma2^{f/f}$ and SSTCre:$\gamma2^{f/f}$ mice in an OFT, we observed an interaction of genotype and stress on distance traveled, with an UCMS-induced increase in locomotion of SSTCre:$\gamma2^{f/f}$ mice but not $\gamma2^{f/f}$ mice (Fig. 3C). The time spent in the center of the OFT remained unchanged (Fig. 3D). The stress-induced hyperactivity of male SSTCre:$\gamma2^{f/f}$ mice then led us to focus the subsequent behavioral analyses on largely locomotion-insensitive behavioral parameters. In the EPM, we observed a genotype effect on percent time spent on open arms, with an anxiolytic-like increase in open arm time in SSTCre:$\gamma2^{f/f}$ vs. $\gamma2^{f/f}$ mice independent of stress (Fig. 3E). This confirms the anxiolytic-like

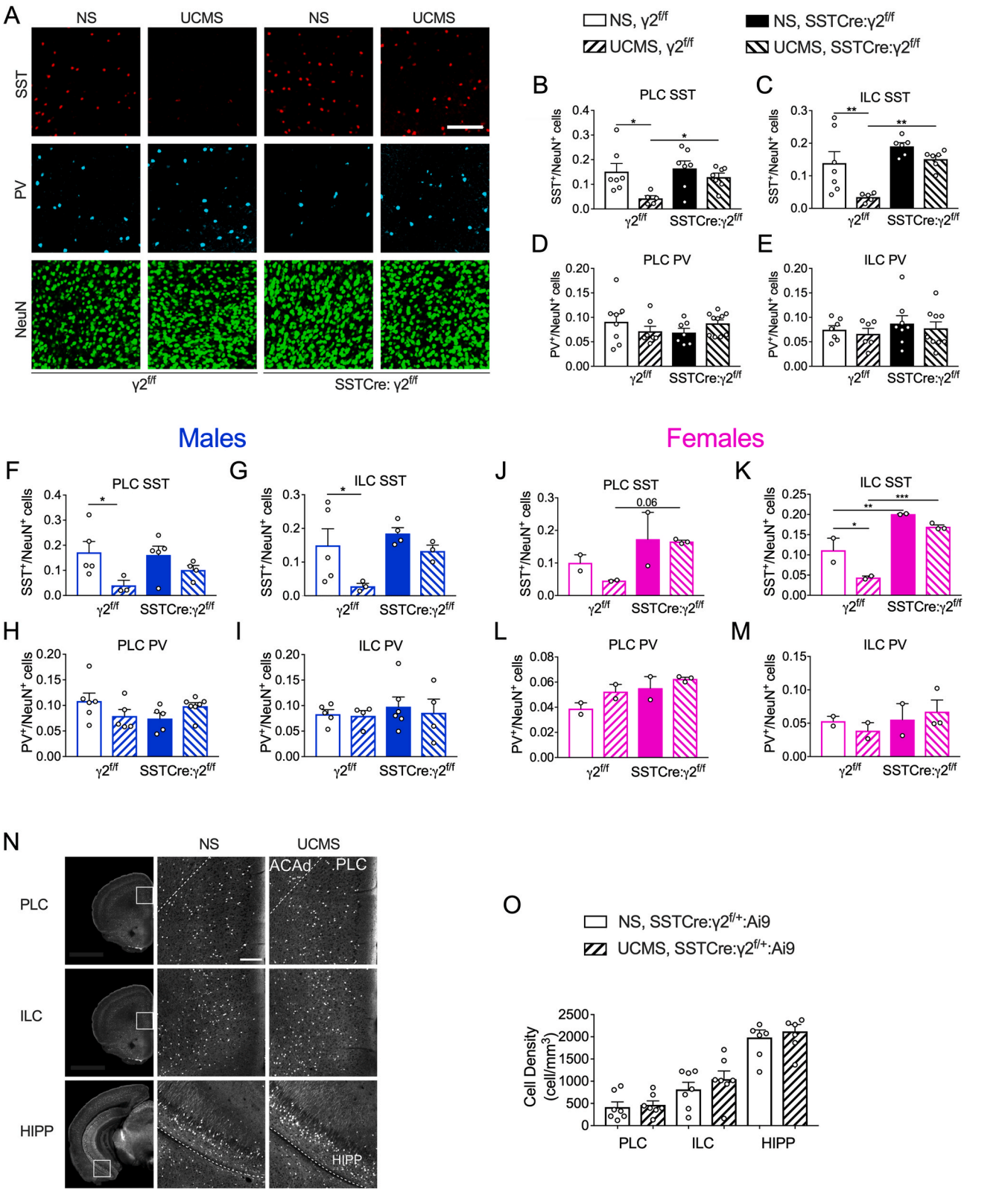

(caption on next page)

Fig. 1. SSTCre:γ2$^{f/f}$ mice are resilient to chronic stress-induced downregulation of SST. A–E) Quantification of SST- and PV-IP interneurons in NS and UCMS-exposed SSTCre:γ2$^{f/f}$ and γ2$^{f/f}$ mice. **A**) Representative micrographs of PLC sections immuno-stained for SST (red), PV (cyan) and NeuN (green). Scale bar, 150 μm. **B-E**) Summary statistics of interneuron densities normalized to NeuN-positive neurons. B) UCMS reduced the density of SST-IP cells in the PLC of γ2$^{f/f}$ mice ($F_{1,\ 22}$ = 7.435, p = 0.012, ANOVA, p = 0.01, Fisher's test) but not SSTCre:γ2$^{f/f}$ mice (p = 0.33). The density of SST-IP cells was greater in UCMS SSTCre:γ2$^{f/f}$ than UCMS γ2$^{f/f}$ mice (p = 0.004). **C**) In the ILC, UCMS reduced the density of SST-IP cells in γ2$^{f/f}$ ($F_{1,20}$ = 9.923, p = 0.005, ANOVA; p = 0.004, Fisher's test) but not SSTCre:γ2$^{f/f}$ mice (p = 0.24). The density of SST-IP cells was greater in UCMS SSTCre:γ2$^{f/f}$ than UCMS γ2$^{f/f}$ mice (p = 0.002). **D,E**) The density of PV-IP cells in the PLC (D) and ILC (E) was unaffected by UCMS and genotype. **F**) In the PLC of males, UCMS reduced the density of SST-IP cells in γ2$^{f/f}$ mice ($F_{1,13}$ = 7.03, p = 0.020, ANOVA; p = 0.028, Fisher's test) but not SSTCre:γ2$^{f/f}$ mice (p = 0.24). **G**) Similarly, in the ILC, UCMS reduced the density of SST-IP cells in γ2$^{f/f}$ ($F_{1,11}$ = 5.44, p = 0.040, ANOVA; p = 0.038, Fisher's LSD) but not SSTCre:γ2$^{f/f}$ mice (p = 0.35). The density of SST-IP cells trended higher in UCMS SSTCre:γ2$^{f/f}$ vs UCMS γ2$^{f/f}$ mice (p = 0.096). **H,I**) The density of PV-IP cells in the PLC (H) and ILC (I) of males was unaffected by UCMS and genotype. **J,K**) The density of SST-IP cells of female mice was increased in SSTCre:γ2$^{f/f}$ vs. γ2$^{f/f}$ mice in both PLC (J) ($F_{1,5}$ = 6.85, p = 0.047) and ILC (K) ($F_{1,5}$ = 65.44, p = 0.0005) with a trend for increased density of SST-IP cells in UCMS SSTCre:γ2$^{f/f}$ vs. UCMS γ2$^{f/f}$ mice (p = 0.06). In the ILC, the density of SST-IP cells was reduced by UCMS ($F_{1,5}$ = 13.86, p = 0.014) and increased in NS SSTCre:γ2$^{f/f}$ vs. NS γ2$^{f/f}$ mice (p = 0.006) and increased in UCMS SSTCre:γ2$^{f/f}$ vs. UCMS γ2$^{f/f}$ mice (p = 0.0009). UCMS selectively reduced the density of SST-IP cells in γ2$^{f/f}$ (p = 0.018) but not SSTCre:γ2$^{f/f}$ mice. **L,M**) The density of PV-IP cells in the PLC (L) and ILC (M) was unaffected by stress (PLC: $F_{1,5}$ = 4.21, p = 0.10; ILC: $F_{1,5}$ = 0.0042, p = 0.95) but increased in PLC of SSTCre:γ2$^{f/f}$ vs. γ2$^{f/f}$ mice. No such genotype effect was evident in the ILC ($F_{1,5}$ = 0.77, p = 0.42). The density of PV-IP cells in the PLC was increased in SSTCre:γ2$^{f/f}$ vs. γ2$^{f/f}$ mice independent of stress ($F_{1,5}$ = 6.67, p = 0.049). **N**) STPT of NS and UCMS SSTCre:γ2$^{f/+}$:Ai9 mice, with micrographs illustrating tdT-positive cells from the PLC, ILC and ventral hippocampus (HIPP). Square insets in the first column of images highlight areas enlarged in the second and third column. Dotted lines demarcate the anterior cingulate cortex (ACAd) from the PLC and the postpiriform transition area from the hippocampus (HIPP), respectively. **O)** Summary data comparing densities of tdT-positive cells in NS vs. UCMS treated SSTCre:γ2$^{f/+}$:Ai9 mice. Scale bar, 200 μm. Data represent 2-way ANOVA and Fisher's test. Graphs represent means ± SE. *p < 0.05, **p < 0.01, ***p < 0.001. For a complete list of ANOVAs and posthoc tests see Supplement 2. (For interpretation of the references to colour in this figure legend, the reader is referred to the Web version of this article.)

phenotype previously reported for the 129 strain of SSTCre:γ2$^{f/f}$ mice (Fuchs et al., 2017). Notably, similar to the OFT the EPM failed to show anxiogenic-like consequences of UCMS in γ2$^{f/f}$ mice (Fig. 3D,E); however, we observed anxiogenic-like effects of UCMS in wildtype (WT) and SSTCre control groups in both of these tests (Figs. S1C and D, Supplement 1). The indistinguishable behavior of WT and SSTCre mice in the OFT and EPM confirmed that the anxiolytic-like phenotype of SSTCre:γ2$^{f/f}$ vs. γ2$^{f/f}$ mice required Cre-mediated recombination of the γ2 locus.

In the NSFT, the latency to feed of γ2$^{f/f}$ and SSTCre:γ2$^{f/f}$ mice showed an overall stress effect and a trend for a stress × genotype interaction (Fig. 3F). Post hoc tests showed an anxiogenic-like increase in latency to feed in UCMS γ2$^{f/f}$ vs. NS γ2$^{f/f}$ mice, but not in UCMS SSTCre:γ2$^{f/f}$ mice vs. NS SSTCre:γ2$^{f/f}$ mice, suggesting resilience of SSTCre:γ2$^{f/f}$ mice to the anxiogenic effects of chronic stress. This phenotype was dependent on Cre-mediated recombination as UCMS increased the latency to feed of SSTCre mice in a manner indistinguishable from WT mice (Fig. S1). Home cage feeding of mice that were food deprived and refed in their home cage remained unaffected by genotype, and UCMS exposed SSTCre:γ2$^{f/f}$ mice ate less rather than more than NS SSTCre:γ2$^{f/f}$ mice (Fig. S2A). Thus, the stress resilient phenotype of SSTCre:γ2$^{f/f}$ mice in the NSFT was not explained by increased appetite.

In the SSPT, we observed an overall stress effect on grooming duration, with UCMS γ2$^{f/f}$ mice spending less time grooming than NS γ2$^{f/f}$ mice. By contrast, grooming behavior of SSTCre:γ2$^{f/f}$ remained unaffected by UCMS (Fig. 4G). However, the grooming duration was unaffected by UCMS also in SSTCre mice (Fig. S1F), suggesting that resilience of SSTCre:γ2$^{f/f}$ mice in this test was independent of *Gabrg2* locus inactivation and the test therefore not informative. Similarly, the SPT showed a small but significant overall stress effect on sucrose preference but post hoc comparisons were not significant and the test therefore not informative (Fig. 3H). Taken together, the data indicate that male SSTCre:γ2$^{f/f}$ are resilient to UCMS-induced reductions in weight gain and UCMS-induced increases in anxiety in the NSFT. Stress resilience could not be assessed in other tests (OFT, EPM, SSPT, SPT) because corresponding behavioral parameters were insensitive to UCMS or because of aberrant behavior of SSTCre control mice.

3.5. SSTCre:γ2$^{f/f}$ female mice differ from males in that they remain sensitive to UCMS-induced anxiety

Female SSTCre:γ2$^{f/f}$ mice showed resilience to UCMS-induced reductions in the density of SST-IP cells, similar to males. However, they differed from males in that they showed a paradoxical UCMS-induced reduction of p-eEF2^{T56} in the mPFC. Female mice (produced as littermates of males tested in Fig. 3) underwent the same UCMS protocol and behavioral tests as the males (Fig. 4A) but were tested on different days within the same week. As for males, we repeated these experiments in a separate cohort of SSTCre and WT littermates, to assess the possible contribution of unspecific Cre effects (Fig. S3). In contrast to males, UCMS did not alter the body weight gain of female mice, independent of genotype (Fig. 4B). In the OFT, female mice showed a genotype effect on locomotion (Fig. 4C). Measurements of center duration revealed an overall anxiogenic effect of UCMS. UCMS significantly decreased the center duration of SSTCre:γ2$^{f/f}$ but not γ2$^{f/f}$ mice, suggesting a chronic stress-induced increase in anxiety selectively in SSTCre:γ2$^{f/f}$ mice (Fig. 4D). Notably, a similar UCMS-induced reduction in center duration was evident also in SSTCre and WT control animals, confirming that SSTCre:γ2$^{f/f}$ mice showed normal sensitivity to stress (Fig. S3C). In the EPM, there was a genotype effect on percent time spent on open arms (Fig. 4E). NS SSTCre:γ2$^{f/f}$ vs. NS γ2$^{f/f}$ mice showed the expected anxiolytic-like phenotype reported previously for the 129 strain of these mice (Fuchs et al., 2017). UCMS-exposed SSTCre:γ2$^{f/f}$ mice vs. UCMS γ2$^{f/f}$ mice showed an anxiolytic-like increase in the time on open arms. This result may indicate stress resilience of female SSTCre:γ2$^{f/f}$ mice but is compromised by absence of significant UCMS effects in γ2$^{f/f}$, WT and SSTCre controls (Fig. 4E and Fig. S3D). In the NSFT, the latency to feed showed a significant effect of stress and a genotype × stress interaction (Fig. 4F). NS SSTCre:γ2$^{f/f}$ mice showed a reduced latency to feed vs. NS γ2$^{f/f}$ mice, as previously seen with the 129 strain of these mice. However, UCMS increased the latency to feed selectively in SSTCre:γ2$^{f/f}$ mice but not γ2$^{f/f}$ mice (Fig. 4F), which indicates enhanced rather than reduced stress sensitivity of the mutants and is opposite to the stress resilient phenotype described in this test for males (Fig. 3F). In the SSPT, there was a stress effect and stress × genotype interaction on grooming duration (Fig. 4G). NS SSTCre:γ2$^{f/f}$ mice showed an increased grooming duration compared to NS γ2$^{f/f}$ mice, suggesting reduced emotionality at baseline as expected based on the same phenotype previously seen with the 129 strain of these mice. UCMS-exposed SSTCre:γ2$^{f/f}$ mice showed reduced grooming duration compared to their NS controls with a similar trend apparent also in UCMS γ2$^{f/f}$ mice vs. NS γ2$^{f/f}$ mice. Thus, SSTCre:γ2$^{f/f}$ female mice remained sensitive to the detrimental effects of UCMS in this test (Fig. 4G). The SPT did not reveal any genotype or stress effects in female mice and therefore was not suitable to assess genotype dependent changes in stress sensitivity (Fig. 4H).

Taken together, SSTCre:γ2$^{f/f}$ female mice differed from males in that they remained susceptible to UCMS in the OFT, SSPT and NSFT. Sex differences were most striking in the NSFT, where male SSTCre:γ2$^{f/f}$ mice were resilient and female SSTCre:γ2$^{f/f}$ mice showed increased susceptible to UCMS. Results for the EPM were ambiguous due to the

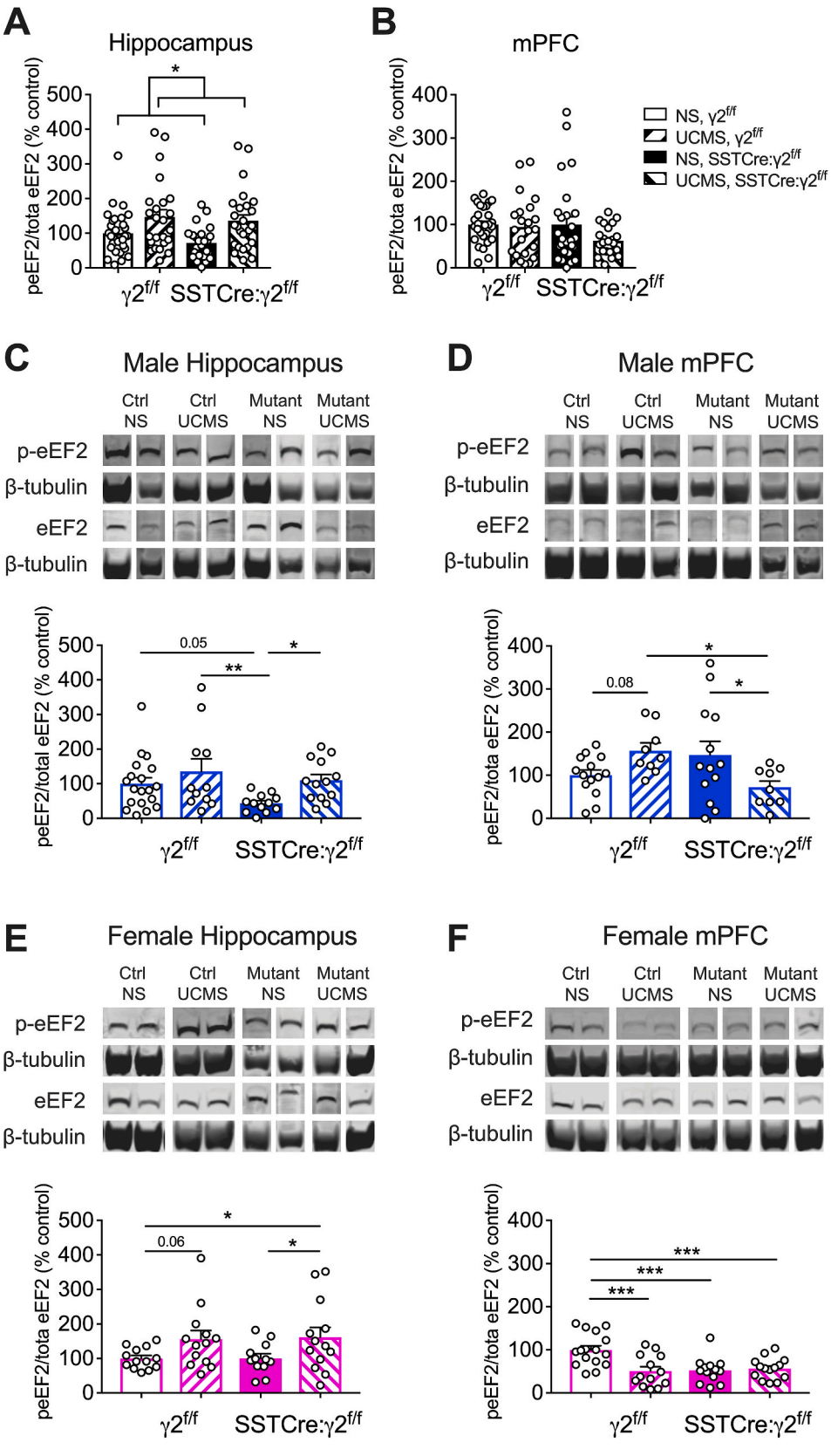

Fig. 2. Male SSTCre:$\gamma2^{f/f}$ mice are resilient to chronic stress-induced increases in eEF2 phosphorylation in mPFC. A,B) UCMS increased p-eEF2^{T56}/eEF2 independent of sex and genotype in the ventral hippocampus (**A**) ($F_{1, 102} = 6.22$, $p = 0.014$) but not mPFC (**B**) ($F_{1, 97} = 2.81$, $p = 0.10$). **C,D) Males:** Representative western blots of male mice and summary statistics of p-eEF2^{T56}/eEF2 in ventral hippocampus and mPFC. In hippocampus (**C**), p-eEF2^{T56}/eEF2 showed a stress effect ($F_{1, 51} = 5.93$, $p = 0.018$). In mPFC (**D**), p-eEF2^{T56}/eEF2 showed an interaction of stress and genotype ($F_{1,41} = 8.63$, $p = 0.005$). UCMS tended to increase p-eEF2^{T56}/eEF2 in $\gamma2^{f/f}$ mice ($p = 0.08$, $n = 9$–14) but reduced this ratio in SSTCre:$\gamma2^{f/f}$ mice ($p = 0.02$, $n = 9$–13). The p-eEF2^{T56} level of UCMS $\gamma2^{f/f}$ mice was increased compared to that of UCMS SSTCre:$\gamma2^{f/f}$ mice ($p = 0.02$, $n = 9$). **E,F) Females**: In hippocampus (**E**), p-eEF2^{T56}/eEF2 showed an overall stress effect ($F_{1,47} = 7.90$, $p = 0.007$) that was almost significant in $\gamma2^{f/f}$ ($p = 0.06$) and significant in SSTCre:$\gamma2^{f/f}$ mice ($p = 0.046$, $n = 12$–13). In mPFC (**F**), the p-eEF2^{T56}/eEF2 ratio showed stress ($F_{1,52} = 6.50$, $p = 0.014$) and genotype effects ($F_{1,52} = 5.77$, $p = 0.020$) and a stress × genotype interaction ($F_{1,52} = 9.16$, $p = 0.004$). NS SSTCre:$\gamma2^{f/f}$ mice vs. NS $\gamma2^{f/f}$ controls showed a paradoxical reduction of p-eEF2^{T56}/eEF2 ($p = 0.0003$, $n = 13$–16). 2-way ANOVAs and Fisher's test. Graphs represent means ± SE. $^{*}p < 0.05$, $^{**}p < 0.01$, $^{***}p < 0.001$.

absence of clear stress effects in $\gamma2^{f/f}$ controls.

4. Discussion

We here have shown that genetic disinhibition of SST cells renders male mice resilient to UCMS across four different levels of analyses.

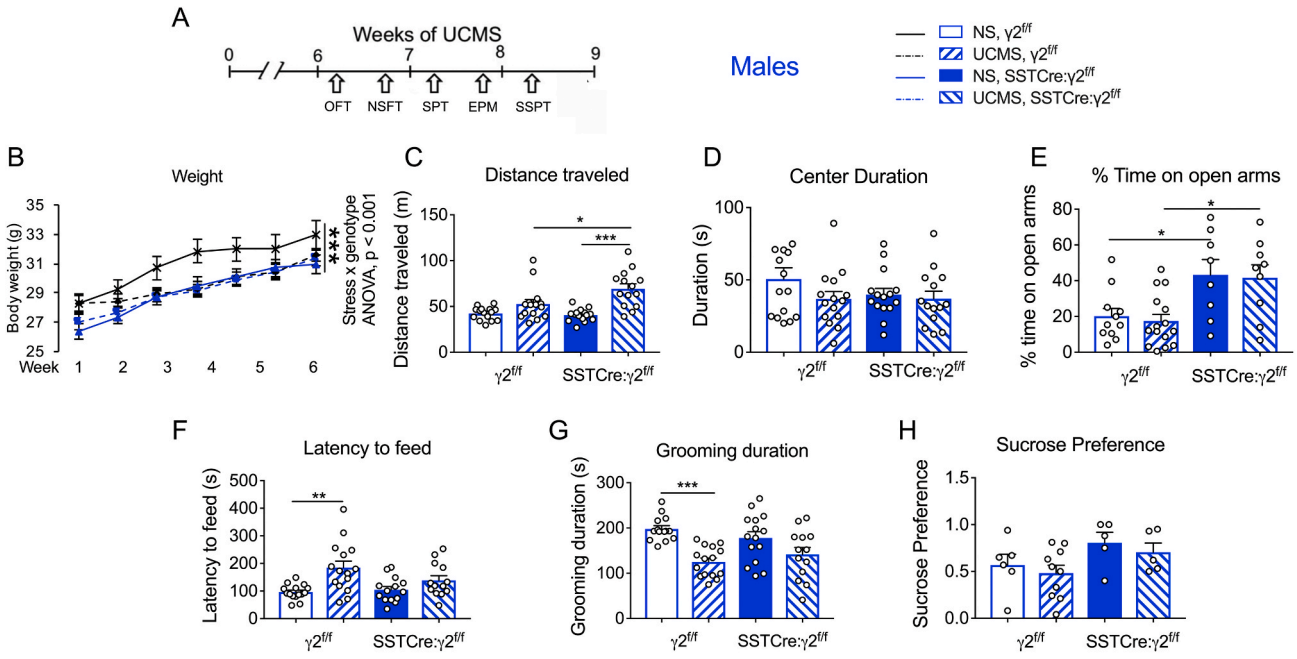

Fig. 3. Male SSTCre:γ2$^{f/f}$ mice are resilient to chronic stress-induced emotional behavior. A) Experimental design. **B**) Male SSTCre:γ2$^{f/f}$ mice were resilient to UCMS-induced reductions in weight gain as evidenced by a stress × genotype interaction ($F_{1,385} = 11.23$, $p < 0.001$, 3-way repeated measurement ANOVA). **C,D**) In the OFT, there was an interaction of stress x genotype in the total distance traveled (C) ($F_{1,55} = 5.969$, $p = 0.018$). UCMS increased locomotion of SSTCre:γ2$^{f/f}$ ($p < 0.001$, $n = 14$–15) and UCMS-exposed SSTCre:γ2$^{f/f}$ showed greater locomotion than UCMS-exposed γ2$^{f/f}$ controls ($p = 0.015$, $n = 14$–15). The center duration (D) was unaffected by stress and genotype. **E**) In the EPM, there was an anxiolytic-like genotype effect on % time spent on open arms ($F_{1,40} = 17.04$, $p < 0.001$), but no stress effect ($F_{1,40} = 0.14$, $p = 0.71$). Post hoc tests confirmed the anxiolytic phenotype of NS SSTCre:γ2$^{f/f}$ mice vs. NS γ2$^{f/f}$ controls ($p = 0.046$, $n = 8$–11) and UCMS SSTCre:γ2$^{f/f}$ mice vs. UCMS γ2$^{f/f}$ controls ($p = 0.016$, $n = 9$–15). **F**) In the NSFT, there was a stress effect on latency to feed ($F_{1,53} = 14.44$, $p < 0.001$) and a trend for a stress × genotype interaction ($F_{1,53} = 2.841$, $p = 0.098$). UCMS increased the latency to feed of γ2$^{f/f}$ mice ($p = 0.0012$, $n = 15$) but not SSTCre:γ2$^{f/f}$ mice ($p = 0.47$, $n = 13$–14). **G**) In the SSPT, there was an overall stress effect ($F_{1,53} = 22.09$, $p < 0.001$). UCMS reduced the grooming duration of γ2$^{f/f}$ ($p < 0.001$, $n = 14$–15) but not SSTCre:γ2$^{f/f}$ mice ($p = 0.14$, $n = 13$–15). **H**) The SPT showed a genotype effect, with a greater sucrose preference in SSTCre:γ2$^{f/f}$ compared to γ2$^{f/f}$ mice ($F_{1,22} = 4.76$, $p = 0.04$). However, post hoc comparisons of NS γ2$^{f/f}$ vs. NS SSTCre:γ2$^{f/f}$ ($p = 0.45$), and UCMS γ2$^{f/f}$ vs. UCMS SSTCre:γ2$^{f/f}$ ($p = 0.41$, $n = 5$–10) were not significant, and there was no UCMS effect ($F_{1,22} = 0.78$, $p = 0.39$), nor a UCMS X genotype interaction ($F_{1,22} = 0.0042$, $p = 0.95$). Data were analyzed by 2-way ANOVA and Tukey test. Bar graphs represent means ± SE. *$p < 0.05$, **$p < 0.01$, ***$p < 0.001$.

Systemically, SSTCre:γ2$^{f/f}$ male mice showed resilience to UCMS-induced reductions in weight gain. At the cell and tissue level of the mPFC, male SSTCre:γ2$^{f/f}$ mice showed resilience to UCMS-induced reductions in SST expression and UCMS-induced increases in p-eEF2. Lastly, at the behavioral level, SSTCre:γ2$^{f/f}$ males were resilient to UCMS-induced increases in anxiety in the NSFT. Notably, behavioral sensitivity to UCMS of γ2$^{f/f}$ controls and resilience to UCMS of SSTCre:γ2$^{f/f}$ mice correlated with bidirectional changes in eEF2 phosphorylation specifically in mPFC but not in hippocampus. In contrast to males, female SSTCre:γ2$^{f/f}$ mice appeared more sensitive to the behavioral effects of UCMS than their γ2$^{f/f}$ controls and they lacked any signs of resilience to UCMS induced changes in eEF2 phosphorylation. Nevertheless, female SSTCre:γ2$^{f/f}$ mice were resilient to UCMS induced reductions in SST-IP cells. Collectively, the data indicate that sex-specific mechanisms underlying vulnerability and resilience to stress map to mPFC rather than hippocampus. Moreover, maintaining the density of SST-IP cells (a measure of SST expression) is insufficient to confer stress resilience to female mice. This is noteworthy, given that SST is consistently downregulated both in chronic stress exposed rodents and postmortem brain of MDD patients (Fee et al., 2020).

We previously showed that stress naïve SSTCre:γ2$^{f/f}$ mice exhibit normal SST mRNA and protein levels, suggesting that the anxiolytic and antidepressant-like phenotype of these mice did not involve altered SST levels (Fuchs et al., 2017). Nevertheless, micro-infusion of SST into brain of mice is known to have anxiolytic and antidepressant-like consequences (Engin et al., 2008). Here we showed that behavioral resilience to UCMS of male SSTCre:γ2$^{f/f}$ mice correlated with stabilized SST expression, which raises the question whether stabilized SST levels or activity-dependent increases in the release of SST contribute to behavioral stress resilience of male SSTCre:γ2$^{f/f}$ mice. Two lines of evidence suggest that this was not the case. First, disinhibition of SST neurons and stabilizing the expression of SST was insufficient to confer behavioral stress resilience to female mice. Second, SST heterozygous mice with correspondingly reduced expression of SST show normal baseline emotional behavior and unaltered UCMS-induced emotional reactivity (Lin and Sibille, 2015), These data suggest that the emotional behavior of mice is insensitive to moderate changes in SST expression and that downregulation of SST in response to stress in mice and in MDD serves merely as a marker of SST neuron dysfunction. Consistent with this interpretation, UCMS results in largely nonoverlapping sex-specific transcriptome changes in SST neurons (Ghosal et al., 2020). Given that SSTCre:γ2$^{f/f}$ mice mimic ketamine-induced potentiation of GABAergic inhibition of pyramidal cells (Ren et al., 2016; Fuchs et al., 2017) and prefrontal reductions in eEF2 phosphorylation (Fuchs et al., 2017), it seems likely that the stress-resilient phenotype of male SSTCre:γ2$^{f/f}$ mice similarly involves enhanced GABAergic inhibition of pyramidal cells.

Our results revealed marked sex-specific effects of SST neuron disinhibition on eEF2 phosphorylation. Increased eEF2 phosphorylation is known to inhibit translation while reduced p-eEF2 is associated with increased dendritic translation (Sutton et al., 2007; Taha et al., 2013). UCMS-induced increases in p-eEF2 are consistent with similar findings described by others in rats (Gronli et al., 2012). Conversely, reduced p-eEF2 levels in male SSTCre:γ2$^{f/f}$ mice are consistent with reduced phosphorylation of eEF2 observed in ketamine treated male mice (Autry et al., 2011; Gideons et al., 2014). Ketamine-induced antidepressant

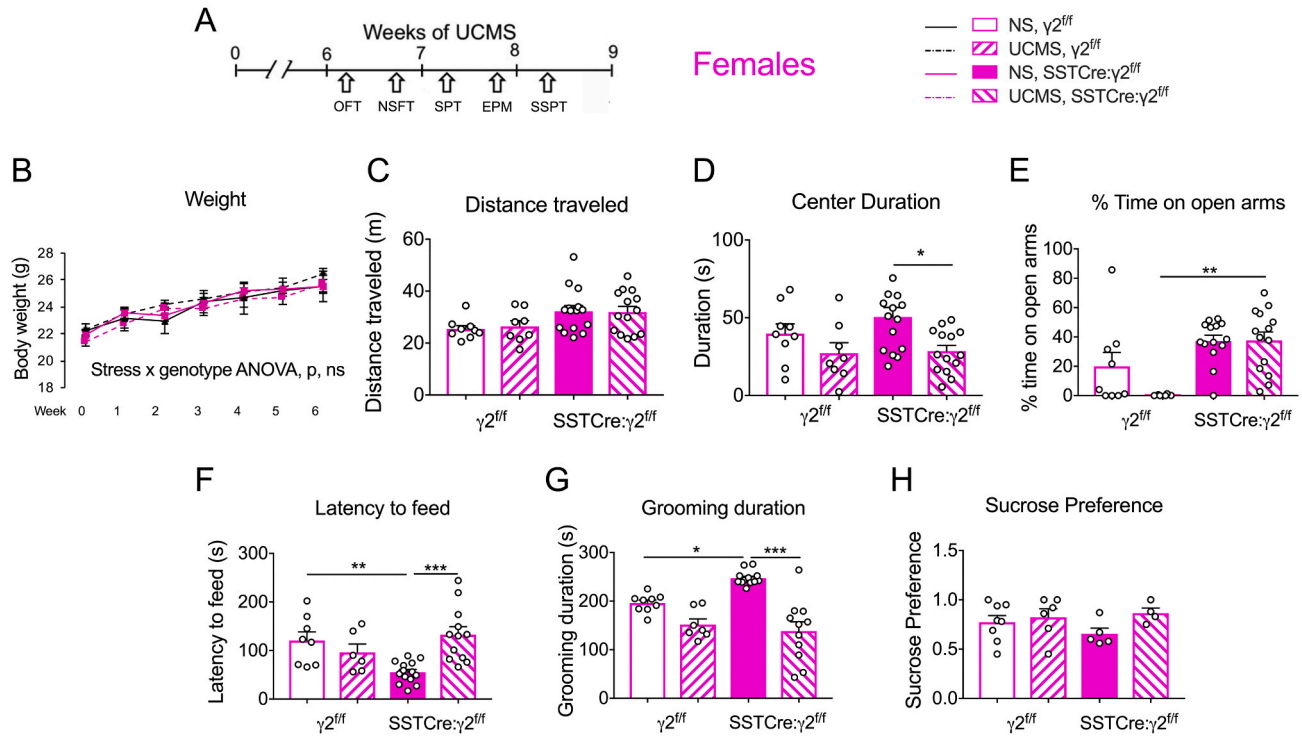

Fig. 4. Female SSTCre:γ2$^{f/f}$ mice do not exhibit behavioral resilience to UCMS. Behavioral analyses of female SSTCre:γ2$^{f/f}$ mice and γ2$^{f/f}$ controls under NS and UCMS conditions. **A**) Experimental design. **B**) Weight gain of female mice was unaffected by UCMS. and genotype (stress x genotype $F_{1,293} = 2.53$, $p = 0.11$, 3-way repeated measurement ANOVA). **C,D**) The distance traveled in the OFT was increased in SSTCre:γ2$^{f/f}$ vs. γ2$^{f/f}$ mice (C) ($F_{1,42} = 7.76$, $p = 0.008$) independent of stress. The center duration (D) showed an anxiogenic effect of UCMS ($F_{1,42} = 8.50$, $p = 0.0057$). UCMS decreased the time spent in the center of SSTCre:γ2$^{f/f}$ ($p = 0.02$, $n =$ 14–15) but not γ2$^{f/f}$ mice ($p = 0.55$, $n =$ 8–9). **E**) In the EPM, SSTCre:γ2$^{f/f}$ vs. γ2$^{f/f}$ mice spent an increased percentage of time on open arms ($F_{1,39} = 14.53$, $p =$ 0.0005) independent of UCMS. **F**) The latency to feed in the NSFT showed a UCMS effect ($F_{1,40} = 4.613$, $p = 0.038$) and a stress × genotype interaction ($F_{1,40} = 12.43$, $p = 0.0011$) with the expected reduction in latency to feed in NS SSTCre:γ2$^{f/f}$ vs. NS γ2$^{f/f}$ mice ($p = 0.009$, $n =$ 9–15) and a reduced feeding latency in UCMS vs. NS SSTCre:γ2$^{f/f}$ mice ($p < 0.001$, $n =$ 13–15) but not UCMS vs. NS γ2$^{f/f}$ mice ($p = 0.73$, $n =$ 8–9). **G**) The SSPT showed a UCMS-induced overall reduction in grooming duration ($F_{1,36} = 39.23$, $p < 0.0001$) and an interaction of stress x genotype effects ($F_{1,36} = 7.053$, $p = 0.0117$). NS SSTCre:γ2$^{f/f}$ mice spent more time grooming than NS γ2$^{f/f}$ mice ($p = 0.017$, $n =$ 9–13), and UCMS reduced the grooming duration in SSTCre:γ2$^{f/f}$ ($p < 0.001$, $n =$ 11–13) but not γ2$^{f/f}$ mice ($p = 0.11$, $n =$ 8–9). **H**) The SPT showed no effects of UCMS and genotype. Data were analyzed by 2-way ANOVA and Tukey test. Bar graphs represent means ± SE. *$p < 0.05$, **$p < 0.01$, ***$p <$ 0.001.

effects are further associated with prominent enhancement of GABAergic synaptic inhibition (Ren et al., 2016; Ghosal et al., 2020). Therefore, our data from male mice suggest that bidirectional changes in synaptic excitation:inhibition ratios resulting from UCMS or SST neuron disinhibition are linked to emotion-related behavioral outcomes by Ca^{2+}-mediated changes in mPFC p-eEF2 levels. No such relationship was evident for female mice.

While tissue measures of p-eEP2 point to sex specific UCMS effects on translation at the tissue level (thought be representative mainly of pyramidal cell dendrites), recent analyses of cell specific transcriptomes by RNAseq has revealed male- and SST neuron-specific activation of the Integrated Stress Response (ISR) pathway, evidenced by prominent downregulation of elongation initiation factor 2 and other ribosomal transcripts representative of this pathway (Lin and Sibille, 2015; Girgenti et al., 2019). Remarkably, the ISR pathway was unaffected in SST neurons of female mice, although they showed overall more numerous gene expression changes than males (Girgenti et al., 2019). Our finding of similar downregulation of SST-IP cells in UCMS-exposed male and female γ2$^{f/f}$ mice therefore suggests that the SST gene is not a target of the ISR pathway.

Stress-induced defects in GABAergic inhibition may be corroborated by altered density or function of PV interneurons, although we found no stress or genotype effects on the density of these neurons. Consistent with our findings, PV neurons show much fewer sex-specific transcript changes that SST neurons (Girgenti et al., 2019) and there is no consensus regarding the contribution of PV neurons to stress vulnerability, with the majority of preclinical studies showing unaltered or downregulated PV neuron densities and one group reporting upregulation by chronic stress (reviewed in Fogaca and Duman, 2019). Similarly, compared to SST neurons, there are few reports pointing to altered PV neuron density in MDD (Sibille et al., 2011).

We noted in the Result section that stress-naive SSTCre:γ2$^{f/f}$ mice of the BL/6J strain only partially replicated the anxiolytic and antidepressant phenotype previously reported for the 129 strain. This may be explained by the recently discovered BL/6J strain-specific hypomorphic allele for the *Gabra2* gene that results in a ~50% reduced expression of α2 $GABA_A$Rs (Mulligan et al., 2019). Hemizygous knockout of this gene in the 129 strain of mice results in heightened anxiety in the NSFT and increased immobility in forced swim and tail suspension tests, respectively (Vollenweider et al., 2011), thereby strongly suggesting that reduced expression of α2 $GABA_A$Rs in BL/6J vs 129 mice contributes to altered baseline emotional behavior of these mice. Moreover, because α2 and γ2 subunits are part of the same $GABA_A$R complex and essential for inhibitory synapse function (Essrich et al., 1998), deletion of the γ2 subunit from SST cells in SSTCre:γ2$^{f/f}$ mice is predicted to result in a lesser degree of disinhibition of these neurons in the BL/6J vs. 129 strain of mice, which explains the less robust anxiolytic and antidepressant phenotype of the BL/6J compared to 129 strain of SSTCre:γ2$^{f/f}$ mice.

In conclusion, enhancing GABAergic inhibition of pyramidal cell dendrites by disinhibition of SST interneurons confers molecular, cellular and behavioral resilience to detrimental effects of stress selectively in male mice. In contrast to males, disinhibition of SST

interneurons protects from UCMS only at the level of SST expression in SST^{+} interneurons, which appears inconsequential for behavioral outcomes. Future experiments will need to address whether, as predicted by the data presented here, disinhibition of SST neurons delimited to mPFC is sufficient to confer resilience and whether resilience is also seen in chronic stress models that consistently lead to anhedonia. Lastly, it will be important to examine whether UCMS effects on the ISR pathway are attenuated in SSTCre:$\gamma 2^{f/f}$ mice and, if they are, whether any such effects are sex and cell-type specific.

Declaration of competing interest

The authors report no study related financial interests or potential conflicts of interest.

CRediT authorship contribution statement

Sarah J. Jefferson: Conceptualization, Formal analysis, Writing - original draft, Writing - review & editing. **Mengyang Feng:** Validation, Formal analysis, Writing - original draft, Writing - review & editing. **URee Chon:** Formal analysis. **Yao Guo:** Investigation. **Yongsoo Kim:** Supervision, Formal analysis. **Bernhard Luscher:** Validation, Conceptualization, Writing - original draft, Writing - review & editing.

Acknowledgments

We thank Fabiola K. Maldonado for technical assistance. We are grateful to Dr. Max Crowley for expert advice on statistical analyses and to Dr. Nicole Crowley for stimulating discussions. This work was supported by the National Institutes of Health (grants MH099851 to B.L., MH116176 to Y.K. and -MH112306 to S.J.J) as well as Tobacco Cure Funds from the Pennsylvania Department of Health to Y.K. Its contents are solely the responsibility of the authors and do not necessarily represent the views of the funding agency.

Appendix A. Supplementary data

Supplementary data to this article can be found online at https://doi.org/10.1016/j.ynstr.2020.100238.

References

Autry, A.E., Adachi, M., Nosyreva, E., Na, E.S., Los, M.F., Cheng, P.F., Kavalali, E.T., Monteggia, L.M., 2011. NMDA receptor blockade at rest triggers rapid behavioural antidepressant responses. Nature 475, 91–95. https://doi.org/10.1038/nature10130.

Banasr, M., Lepack, A., Fee, C., Duric, V., Maldonado-Aviles, J., DiLeone, R., Sibille, E., Duman, R.S., Sanacora, G., 2017. Characterization of GABAergic marker expression in the chronic unpredictable stress model of depression. Chronic Stress 1, 1–13. https://doi.org/10.1177/2470547017720459. Thousand Oaks.

Bhagwagar, Z., Wylezinska, M., Taylor, M., Jezzard, P., Matthews, P.M., Cowen, P.J., 2004. Increased brain GABA concentrations following acute administration of a selective serotonin reuptake inhibitor. Am. J. Psychiatr. 161, 368–370. https://doi.org/10.1176/appi.ajp.161.2.368.

Chiu, C.Q., Lur, G., Morse, T.M., Carnevale, N.T., Ellis-Davies, G.C., Higley, M.J., 2013. Compartmentalization of GABAergic inhibition by dendritic spines. Science 340, 759–762. https://doi.org/10.1126/science.1234274.

Crestani, F., Lorez, M., Baer, K., Essrich, C., Benke, D., Laurent, J.P., Belzung, C., Fritschy, J.M., Luscher, B., Mohler, H., 1999. Decreased GABAA-receptor clustering results in enhanced anxiety and a bias for threat cues. Nat. Neurosci. 2, 833–839. https://doi.org/10.1038/12207.

Czeh, B., Varga, Z.K., Henningsen, K., Kovacs, G.L., Miseta, A., Wiborg, O., 2015. Chronic stress reduces the number of GABAergic interneurons in the adult rat hippocampus, dorsal-ventral and region-specific differences. Hippocampus 25, 393–405. https://doi.org/10.1002/hipo.22382.

Earnheart, J.C., Schweizer, C., Crestani, F., Iwasato, T., Itohara, S., Mohler, H., Luscher, B., 2007. GABAergic control of adult hippocampal neurogenesis in relation to behavior indicative of trait anxiety and depression states. J. Neurosci. 27, 3845–3854. https://doi.org/10.1523/JNEUROSCI.3609-06.2007.

Elizalde, N., Gil-Bea, F.J., Ramirez, M.J., Aisa, B., Lasheras, B., Del Rio, J., Tordera, R.M., 2008. Long-lasting behavioral effects and recognition memory deficit induced by chronic mild stress in mice: effect of antidepressant treatment. Psychopharmacology 199, 1–14. https://doi.org/10.1007/s00213-007-1035-1.

Engin, E., Stellbrink, J., Treit, D., Dickson, C.T., 2008. Anxiolytic and antidepressant effects of intracerebroventricularly administered somatostatin: behavioral and neurophysiological evidence. Neuroscience 157, 666–676. https://doi.org/10.1016/j.neuroscience.2008.09.037.

Essrich, C., Lorez, M., Benson, J.A., Fritschy, J.M., Luscher, B., 1998. Postsynaptic clustering of major GABAA receptor subtypes requires the gamma 2 subunit and gephyrin. Nat. Neurosci. 1, 563–571. https://doi.org/10.1038/2798.

Fee, C., Banasr, M., Sibille, E., 2017. Somatostatin-positive gamma-aminobutyric acid interneuron deficits in depression: cortical microcircuit and therapeutic perspectives. Biol. Psychiatr. 82, 549–559. https://doi.org/10.1016/j.biopsych.2017.05.024.

Fee C, Prevot T, Misquitta K, Banasr M, Sibille E (2020). doi: 10.1101/2020.02.19.956672.

Fogaca, M.V., Duman, R.S., 2019. Cortical GABAergic dysfunction in stress and depression: new insights for therapeutic interventions. Front. Cell. Neurosci. 13, 87. https://doi.org/10.3389/fncel.2019.00087.

Fuchs, T., Jefferson, S.J., Hooper, A., Yee, P.H., Maguire, J., Luscher, B., 2017. Disinhibition of somatostatin-positive GABAergic interneurons results in an anxiolytic and antidepressant-like brain state. Mol. Psychiatr. 22, 920–930. https://doi.org/10.1038/mp.2016.188.

Ghosal, S., Hare, B., Duman, R.S., 2017. Prefrontal cortex GABAergic deficits and circuit dysfunction in the pathophysiology and treatment of chronic stress and depression. Curr Opin Behav Sci 14, 1–8. https://doi.org/10.1016/j.cobeha.2016.09.012.

Ghosal, S., Duman, C.H., Liu, R.J., Wu, M., Terwilliger, R., Girgenti, M.J., Wohleb, E., Fogaca, M.V., Teichman, E.M., Hare, B., Duman, R.S., 2020. Ketamine rapidly reverses stress-induced impairments in GABAergic transmission in the prefrontal cortex in male rodents. Neurobiol. Dis. 134, 104669. https://doi.org/10.1016/j.nbd.2019.104669.

Gideons, E.S., Kavalali, E.T., Monteggia, L.M., 2014. Mechanisms underlying differential effectiveness of memantine and ketamine in rapid antidepressant responses. Proc. Natl. Acad. Sci. U. S. A. 111, 8649–8654. https://doi.org/10.1073/pnas.1323920111.

Girgenti, M.J., Wohleb, E.S., Mehta, S., Ghosal, S., Fogaca, M.V., Duman, R.S., 2019. Prefrontal cortex interneurons display dynamic sex-specific stress-induced transcriptomes. Transl. Psychiatry 9, 292. https://doi.org/10.1038/s41398-019-0642-z.

Gronli, J., Dagestad, G., Milde, A.M., Murison, R., Bramham, C.R., 2012. Post-transcriptional effects and interactions between chronic mild stress and acute sleep deprivation: regulation of translation factor and cytoplasmic polyadenylation element-binding protein phosphorylation. Behav. Brain Res. 235, 251–262. https://doi.org/10.1016/j.bbr.2012.08.008.

He, M., Tucciarone, J., Lee, S., Nigro, M.J., Kim, Y., Levine, J.M., Kelly, S.M., Krugikov, I., Wu, P., Chen, Y., Gong, L., Hou, Y., Osten, P., Rudy, B., Huang, Z.J., 2016. Strategies and tools for combinatorial targeting of GABAergic neurons in mouse cerebral cortex. Neuron 91, 1228–1243. https://doi.org/10.1016/j.neuron.2016.08.021.

Heise, C., et al., 2016. eEF2K/eEF2 pathway controls the excitation/inhibition balance and susceptibility to epileptic seizures. Cerebr. Cortex. https://doi.org/10.1093/cercor/bhw075.

Isingrini, E., Camus, V., Le Guisquet, A.M., Pingaud, M., Devers, S., Belzung, C., 2010. Association between repeated unpredictable chronic mild stress (UCMS) procedures with a high fat diet: a model of fluoxetine resistance in mice. PloS One 5, e10404. https://doi.org/10.1371/journal.pone.0010404.

Kapfer, C., Glickfeld, L.L., Atallah, B.V., Scanziani, M., 2007. Supralinear increase of recurrent inhibition during sparse activity in the somatosensory cortex. Nat. Neurosci. 10, 743–753. https://doi.org/10.1038/nn1909.

Kim, Y., Venkataraju, K.U., Pradhan, K., Mende, C., Taranda, J., Turaga, S.C., Arganda-Carreras, I., Ng, L., Hawrylycz, M.J., Rockland, K.S., Seung, H.S., Osten, P., 2015. Mapping social behavior-induced brain activation at cellular resolution in the mouse. Cell Rep. 10, 292–305. https://doi.org/10.1016/j.celrep.2014.12.014.

Kim, Y., Yang, G.R., Pradhan, K., Venkataraju, K.U., Bota, M., Garcia Del Molino, L.C., Fitzgerald, G., Ram, K., He, M., Levine, J.M., Mitra, P., Huang, Z.J., Wang, X.J., Osten, P., 2017. Brain-wide maps reveal stereotyped cell-type-based cortical architecture and subcortical sexual dimorphism. Cell 171, 456–469 e422. https://doi.org/10.1016/j.cell.2017.09.020.

Kolata, S.M., Nakao, K., Jeevakumar, V., Farmer-Alroth, E.L., Fujita, Y., Bartley, A.F., Jiang, S.Z., Rompala, G.R., Sorge, R.E., Jimenez, D.V., Martinowich, K., Mateo, Y., Hashimoto, K., Dobrunz, L.E., Nakazawa, K., 2018. Neuropsychiatric phenotypes produced by GABA reduction in mouse cortex and Hippocampus. Neuropsychopharmacology 43, 1445–1456. https://doi.org/10.1038/npp.2017.296.

Kucukibrahimoglu, E., Saygin, M.Z., Caliskan, M., Kaplan, O.K., Unsal, C., Goren, M.Z., 2009. The change in plasma GABA, glutamine and glutamate levels in fluoxetine- or S-citalopram-treated female patients with major depression. Eur. J. Clin. Pharmacol. 65, 571–577. https://doi.org/10.1007/s00228-009-0650-7.

Lau, A., Tymianski, M., 2010. Glutamate receptors, neurotoxicity and neurodegeneration. Pflügers Archiv 460, 525–542. https://doi.org/10.1007/s00424-010-0809-1.

Lin, L.C., Sibille, E., 2015. Somatostatin, neuronal vulnerability and behavioral emotionality. Mol. Psychiatr. 20, 377–387. https://doi.org/10.1038/mp.2014.184.

Lister, R.G., 1987. The use of a plus-maze to measure anxiety in the mouse. Psychopharmacology 92, 180–185.

Liu, X., Carter, A.G., 2018. Ventral hippocampal inputs preferentially drive corticocortical neurons in the infralimbic prefrontal cortex. J. Neurosci. 38, 7351–7363. https://doi.org/10.1523/JNEUROSCI.0378-18.2018.

Luscher, B., Fuchs, T., 2015. GABAergic control of depression-related brain states. Adv. Pharmacol. 73, 97–144. https://doi.org/10.1016/bs.apha.2014.11.003.
Luscher, B., Feng, M., Jefferson, S.J., 2020. Antidepressant mechanisms of ketamine: focus on GABAergic inhibition. Adv. Pharmacol. 89, 43–78. https://doi.org/10.1016/bs.apha.2020.03.002.
Ma, K., Xu, A., Cui, S., Sun, M.R., Xue, Y.C., Wang, J.H., 2016. Impaired GABA synthesis, uptake and release are associated with depression-like behaviors induced by chronic mild stress. Transl. Psychiatry 6, e910. https://doi.org/10.1038/tp.2016.181.
McEwen, B.S., Nasca, C., Gray, J.D., 2016. Stress effects on neuronal structure: Hippocampus, amygdala, and prefrontal cortex. Neuropsychopharmacology 41, 3–23. https://doi.org/10.1038/npp.2015.171.
McNaughton, N., Kocsis, B., Hajos, M., 2007. Elicited hippocampal theta rhythm: a screen for anxiolytic and procognitive drugs through changes in hippocampal function? Behav. Pharmacol. 18, 329–346. https://doi.org/10.1097/FBP.0b013e3282ee82e3.
Moghaddam, B., Jackson, M., 2004. Effect of stress on prefrontal cortex function. Neurotox. Res. 6, 73–78. https://doi.org/10.1007/BF03033299.
Muller, C., Remy, S., 2014. Dendritic inhibition mediated by O-LM and bistratified interneurons in the hippocampus. Front. Synaptic Neurosci. 6, 23. https://doi.org/10.3389/fnsyn.2014.00023.
Mulligan, M.K., Abreo, T., Neuner, S.M., Parks, C., Watkins, C.E., Houseal, M.T., Shapaker, T.M., Hook, M., Tan, H., Wang, X., Ingels, J., Peng, J., Lu, L., Kaczorowski, C.C., Bryant, C.D., Homanics, G.E., Williams, R.W., 2019. Identification of a functional non-coding variant in the GABA A receptor alpha2 subunit of the C57BL/6J mouse reference genome: major implications for neuroscience Research. Front. Genet. 10, 188. https://doi.org/10.3389/fgene.2019.00188.
Newton, D.F., Fee, C., Nikolova, Y.S., Sibille, E., 2019. Altered GABAergic function, cortical microcircuitry, and information processing in depression. In: Quevedo, J., Carvalho, A.F., Zarate, C.A. (Eds.), Neurobiology of Depression. Academic Press, pp. 315–329.
Nosyreva, E., Szabla, K., Autry, A.E., Ryazanov, A.G., Monteggia, L.M., Kavalali, E.T., 2013. Acute suppression of spontaneous neurotransmission drives synaptic potentiation. J. Neurosci. 33, 6990–7002. https://doi.org/10.1523/JNEUROSCI.4998-12.2013.
Opal, M.D., Klenotich, S.C., Morais, M., Bessa, J., Winkle, J., Doukas, D., Kay, L.J., Sousa, N., Dulawa, S.M., 2014. Serotonin 2C receptor antagonists induce fast-onset antidepressant effects. Mol. Psychiatr. 19, 1106–1114. https://doi.org/10.1038/mp.2013.144.
Ren, Z., Pribiag, H., Jefferson, S.J., Shorey, M., Fuchs, T., Stellwagen, D., Luscher, B., 2016. Bidirectional homeostatic regulation of a depression-related brain state by gamma-aminobutyric acidergic deficits and ketamine treatment. Biol. Psychiatr. 80, 457–468. https://doi.org/10.1016/j.biopsych.2016.02.009.
Rudy, B., Fishell, G., Lee, S., Hjerling-Leffler, J., 2011. Three groups of interneurons account for nearly 100% of neocortical GABAergic neurons. Dev Neurobiol 71, 45–61. https://doi.org/10.1002/dneu.20853.
Sanacora, G., Mason, G.F., Rothman, D.L., Krystal, J.H., 2002. Increased occipital cortex GABA concentrations in depressed patients after therapy with selective serotonin reuptake inhibitors. Am. J. Psychiatr. 159, 663–665. https://doi.org/10.1176/appi.ajp.159.4.663.
Schweizer, C., Balsiger, S., Bluethmann, H., Mansuy, I.M., Fritschy, J.M., Mohler, H., Luscher, B., 2003. The gamma 2 subunit of GABA(A) receptors is required for maintenance of receptors at mature synapses. Mol. Cell. Neurosci. 24, 442–450. https://doi.org/10.1016/s1044-7431(03)00202-1.
Shen, Q., Fuchs, T., Sahir, N., Luscher, B., 2012. GABAergic control of critical developmental periods for anxiety- and depression-related behavior in mice. PloS One 7, e47441. https://doi.org/10.1371/journal.pone.0047441.
Shen, Q., Lal, R., Luellen, B.A., Earnheart, J.C., Andrews, A.M., Luscher, B., 2010. gamma-Aminobutyric acid-type A receptor deficits cause hypothalamic-pituitary-adrenal axis hyperactivity and antidepressant drug sensitivity reminiscent of melancholic forms of depression. Biol. Psychiatr. 68, 512–520. https://doi.org/10.1016/j.biopsych.2010.04.024.
Sibille, E., Morris, H.M., Kota, R.S., Lewis, D.A., 2011. GABA-related transcripts in the dorsolateral prefrontal cortex in mood disorders. Int. J. Neuropsychopharmacol. 14, 721–734. https://doi.org/10.1017/S1461145710001616.
Soumier, A., Sibille, E., 2014. Opposing effects of acute versus chronic blockade of frontal cortex somatostatin-positive inhibitory neurons on behavioral emotionality in mice. Neuropsychopharmacology 39, 2252–2262. https://doi.org/10.1038/npp.2014.76.
Stroud, C.B., Davila, J., Hammen, C., Vrshek-Schallhorn, S., 2011. Severe and nonsevere events in first onsets versus recurrences of depression: evidence for stress sensitization. J. Abnorm. Psychol. 120, 142–154. https://doi.org/10.1037/a0021659.
Sutton, M.A., Taylor, A.M., Ito, H.T., Pham, A., Schuman, E.M., 2007. Postsynaptic decoding of neural activity: eEF2 as a biochemical sensor coupling miniature synaptic transmission to local protein synthesis. Neuron 55, 648–661. https://doi.org/10.1016/j.neuron.2007.07.030.
Taha, E., Gildish, I., Gal-Ben-Ari, S., Rosenblum, K., 2013. The role of eEF2 pathway in learning and synaptic plasticity. Neurobiol. Learn. Mem. 105, 100–106. https://doi.org/10.1016/j.nlm.2013.04.015.
Tan, Z., Hu, H., Huang, Z.J., Agmon, A., 2008. Robust but delayed thalamocortical activation of dendritic-targeting inhibitory interneurons. Proc. Natl. Acad. Sci. U. S. A. 105, 2187–2192. https://doi.org/10.1073/pnas.0710628105.
Treadway, M.T., Waskom, M.L., Dillon, D.G., Holmes, A.J., Park, M.T.M., Chakravarty, M.M., Dutra, S.J., Polli, F.E., Iosifescu, D.V., Fava, M., Gabrieli, J.D.E., Pizzagalli, D.A., 2015. Illness progression, recent stress, and morphometry of hippocampal subfields and medial prefrontal cortex in major depression. Biol. Psychiatr. 77, 285–294. https://doi.org/10.1016/j.biopsych.2014.06.018.
Veeraiah, P., Noronha, J.M., Maitra, S., Bagga, P., Khandelwal, N., Chakravarty, S., Kumar, A., Patel, A.B., 2014. Dysfunctional glutamatergic and gamma-aminobutyric acidergic activities in prefrontal cortex of mice in social defeat model of depression. Biol. Psychiatr. 76, 231–238. https://doi.org/10.1016/j.biopsych.2013.09.024.
Vollenweider, I., Smith, K.S., Keist, R., Rudolph, U., 2011. Antidepressant-like properties of alpha2-containing GABA(A) receptors. Behav. Brain Res. 217, 77–80. https://doi.org/10.1016/j.bbr.2010.10.009.
Yavorska, I., Wehr, M., 2016. Somatostatin-expressing inhibitory interneurons in cortical circuits. Front. Neural Circ. 10, 76. https://doi.org/10.3389/fncir.2016.00076.
Zanos, P., Moaddel, R., Morris, P.J., Georgiou, P., Fischell, J., Elmer, G.I., Alkondon, M., Yuan, P., Pribut, H.J., Singh, N.S., Dossou, K.S., Fang, Y., Huang, X.P., Mayo, C.L., Wainer, I.W., Albuquerque, E.X., Thompson, S.M., Thomas, C.J., Zarate Jr., C.A., Gould, T.D., 2016. NMDAR inhibition-independent antidepressant actions of ketamine metabolites. Nature 533, 481–486. https://doi.org/10.1038/nature17998.